Chapter 1
The Basis of Nanomagnetism

Summary. What is the origin of the observed differences in magnetic behavior between a sample with nanometric dimensions and a macroscopic sample of the same material? These differences are shown to arise from broken translation symmetry in nanometric samples, from the higher proportion of atoms on the surface, or interface, from the fact that the sizes of objects of nanoscopic scale, or nanoscale are comparable to some fundamental or characteristic lengths of the constituent material and other effects. The exchange length and the magnetic domain wall width are some of the characteristic lengths that are more relevant to the magnetic properties. The shape of the density of electronic states curve is also dependent on the dimensionality of the samples.

1.1 Introduction: The Importance of Nanomagnetism

The objects of study of Nanoscience are the phenomena involving objects of dimensions usually in the range from 1 nm (1 nm $= 10^{-9}$ m) to 100 nm. This is the range of sizes of many molecules and viruses and is also the characteristic length scale of many physical processes. The lateral dimensions of the present-day integrated circuit components, as well as the dimensions of grains in magnetic recording film media, are contained in this range.

Nanomagnetism is the area of research in Physics that deals with the magnetic properties of objects that have at least one dimension in the nanoscopic range. Nanomagnetism includes in its scope the study of properties and applications of the magnetism of isolated nanoparticles, nanodots, nanowires, thin films and multilayers, and also macroscopic samples that contain nanoscale particles. Materials that contain particles, films, and other structures in the nanometric scale are often described as nanostructured materials.

A.P. Guimarães, *Principles of Nanomagnetism*, NanoScience and Technology,
DOI 10.1007/978-3-319-59409-5_1

Objects with dimensions from 100 to 1000 nm are usually described as mesoscopic; although our focus in the present work is on magnetic properties of objects of nanoscopic dimension, we will also consider the behavior of objects of mesoscopic size.

Nanomagnetism has many practical applications, from geology to magnetic recording, from ferrofluids [28] used in loudspeakers to small particles used in medicine, that can be directed to specific organs and tissues, either for drug delivery [1] or for the application of the technique of magnetic hyperthermia [19].

Magnetic nanoparticles are present in many rocks and soils. The alignment of their magnetic moments under the influence of the geomagnetic field allows the study of the evolution of Earth's magnetism and the determination of their age; this alignment can also inform on past anthropic activities [14].

Nanoparticles of magnetic materials, usually of magnetite, also occur in living beings; perhaps, the best studied example is that of magnetotactic bacteria, which, through magnetic grains of nanometric dimension, align themselves in the Earth's magnetic field. These grains are synthesized by the bacteria, in a process called biomineralization. These magnetic nanoparticles, and the bacteria themselves, have been studied as drug carriers in cancer therapy and other applications [26]. Nanomagnets have also been found in insects, birds, and other creatures [39]. Magnetic particles have been found in the beak and inner ear of pigeons, and they seem to be responsible for part of the birds' ability to detect magnetic fields [30, 40].

Finally, the most successful application of nanomagnetism has been to magnetic recording that has taken this technology through a swift evolution in the last five decades. This is measured by the evolution of the areal bit density in magnetic hard disks that has increased by a factor of many tens of millions since the introduction in the market of this technology (Fig. 1.1) (e.g., [38]). The rapid increase in the density of electronic circuits made on individual silicon chips that has doubled every eighteen months is a tendency known as Moore's Law, a name arising from a 1965 paper by G.E. Moore that discussed the subject. Alongside this evolution, the density of magnetic storage in hard disks, measured by the data areal density, has progressed even faster, doubling every two months.

In order to reach higher and higher storage densities, a great effort was necessary in the study of the properties of small magnetic particles and also of the magnetic thin films that are a constitutive part of hard disk platters and magnetic read heads.

The application to devices, particularly spintronic devices, has represented another frontier in rapid expansion (e.g., [16]). This application is based on the interaction of the spin degree of freedom of an electric current with the magnetic materials and also uses films and other structures with nanometric dimensions.

1.2 The Origin of Nanomagnetic Behavior

The emergence of the new phenomena that are the object of nanomagnetism has its origin in the fact that the magnetism of samples of nanoscopic or mesoscopic sizes presents important differences compared to the magnetism of macroscopic

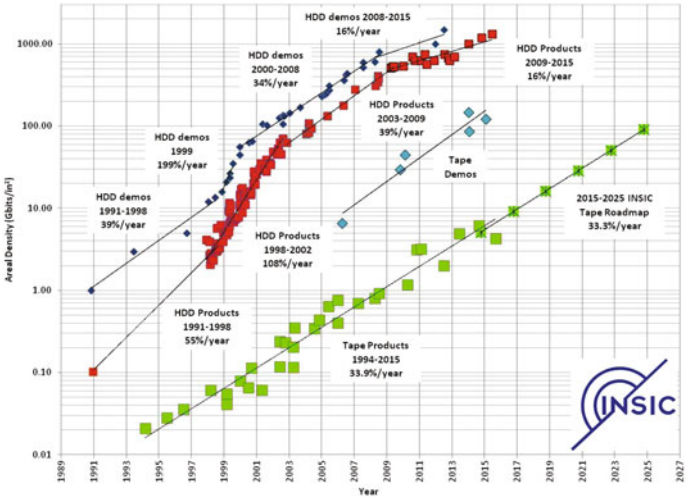

Fig. 1.1 Evolution of magnetic recording: hard disk areal density in Gigabits per square inch as a function of the year (1 Gbit/in^2=0.1550 Gbit/cm^2). Courtesy of the Information Storage Industry Consortium (INSIC)

samples. One could describe these differences, in a simplified way, as arising from the fact that the magnetic systems of nanoscopic or mesoscopic scales present the following: (a) dimensions comparable to characteristic lengths, such as the limiting size of magnetic domains; (b) broken translation symmetry, which results in sites with reduced coordination number, with broken exchange bonds and frustration. Also, nanoscopic or mesoscopic objects exhibit a higher proportion of surface (or interface) atoms.

Another factor that modifies the magnetic properties of the nano-objects is that they are in general in close contact with other physical systems, for example, with a substrate or a capping layer, in the case of most thin films and multilayers. In the case of nanoparticles, these objects may be immersed in solid matrices or compacted in a container: In both cases, each particle may feel a strong interaction with its immediate neighborhood.

Also, in general, as systems such as ensembles of nanoparticles are prepared with smaller dimensions, the importance of imperfections and defects becomes more relevant, making the obtention of identical sets of nano-objects more difficult. Often the properties of nanoscale objects have to be derived from samples formed of ensembles of such objects.

The spin wave spectra of samples of nanoscopic dimensions are also modified (e.g., [22]). The dispersion relation for spin waves for wavelengths longer than the lattice spacing is $\hbar\omega = Dk^2$, where D is the stiffness constant and k is the magnitude of the spin wavevector. For a spin wave energy comparable to the thermal energy, one has $k \approx (k_B T/D)^{1/2}$, where k_B is the Boltzmann constant. For Fe, $D(4.2\,K) \approx 3$ mev nm^2 and the corresponding length $L = 1/k \approx 3$ nm at liquid helium temperature,

Table 1.1 Some characteristic lengths in magnetism and their typical magnitudes

Symbol	Length	Typical magnitude (nm)
d_a	Interatomic distance (Fe)	2.5×10^{-1}
d_{ex}	Range of exchange interaction	$\sim10^{-1}$ to ~1
d_{RKKY}	Range of RKKY interaction	$\sim10^{-1}$ to ~10
d_c	Domain size	10 to 10^4
$D_{\text{cr}}^{\text{spm}}$	Superparamagnetic critical diameter	~1 to $\sim10^2$
$D_{\text{cr}}^{\text{sd}}$	Critical single-domain diameter	~10 to $\sim10^3$
δ_0	Domain wall width	~1 to $\sim10^2$
l_{ex}	Exchange length	~1 to $\sim10^2$
l_{sd}	Spin diffusion length	~10 to 10^2
λ_{mfp}	Electron mean free path	~1 to 10^2
ζ	Superconducting coherence length	$\sim$ 1 to 10^3
λ_F	Fermi wavelength/metal	$\sim10^{-1}$
λ_F	Fermi wavelength/semiconductor	$\sim10^2$

which implies that spin wave spectra of nanoscale objects are significantly modified, if compared to those of bulk samples.

The dynamic behavior of magnetic objects of nanometric size also differs from the behavior of macroscopic samples of the same constituents. The main cause for this difference is the enhanced importance of thermal fluctuations under the usual experimental conditions. The phenomenon of superparamagnetism is observed in magnetic nanoparticles if the thermal energy k_BT is of the same order of magnitude of the anisotropy energy of the particles, leading to an effectively zero measured magnetic moment, in the absence of a magnetic field. The superparamagnetism of nanoparticles is discussed in Sect. 3.3 (p. 82).

1.2.1 Sample Dimensions and Characteristic Lengths

The simplest example of the effect of the characteristic lengths on the magnetic properties is the case of magnetic particles that have dimensions smaller than the critical magnetic single-domain diameter. These particles therefore have the single domain as their lowest energy configuration.

Some of these characteristic lengths, which include the exchange interaction length, the domain wall width, and the spin diffusion length, are given in Table 1.1, together with their typical values. From this table, it is evident that nano-objects have dimensions in the range of many of these characteristic lengths. The derivation of the expressions for some of these lengths, in terms of the magnetic parameters of the constituent materials, will be discussed in Chap. 2.

The critical size for magnetic domains $D_{\text{cr}}^{\text{sd}}$, which is the largest size that a ferromagnetic particle may have, beyond which it will be energetically more favorable to divide itself into two or more domains, varies from material to material. This size varies from about 10 nm to some thousands of nanometers (or microns); some values of this dimension for spherical particles for different materials are shown in Table 2.10, on p. 45. This critical diameter is given by the following expression, to be demonstrated in Chap. 2 (p. 58):

$$D_{\text{cr}}^{\text{sd}} = \frac{72\sqrt{AK}}{\mu_0 M_s^2} \,. \tag{1.1}$$

In this expression, A is the exchange stiffness constant, or parameter, K is the uniaxial anisotropy constant (assumed > 0), M_s is the saturation magnetization, and μ_0 is the vacuum magnetic permeability (or magnetic constant), equal to $4\pi \times 10^{-7}$ H/m in the SI.

The characteristic lengths that are more relevant in defining the magnetic properties of nano-objects are the exchange length and the domain wall width parameter. The exchange length is given by:

$$l_{\text{ex}} = \sqrt{\frac{2A}{\mu_0 M_s^2}} \,. \tag{1.2}$$

Table 1.2 illustrates the magnitude of the exchange length l_{ex} with some examples from the 3d metals.

The domain wall width parameter Δ characterizes the width of the transition region between two magnetic domains, as will be discussed in Chap. 2. It is given as a function of the exchange stiffness constant A and the uniaxial anisotropy constant K, by

$$\Delta = \sqrt{\frac{A}{K}} \,. \tag{1.3}$$

And the domain wall width δ_0 is given by:

$$\delta_0 = \pi \, \Delta \,. \tag{1.4}$$

The domain wall energy is also related to the same parameters A and K. In the simple case of a 180° wall of a cubic crystal, the energy per unit area of the wall is:

$$\gamma = 4\sqrt{AK} \,. \tag{1.5}$$

In Chap. 2, where the properties of magnetic domains are studied, Table 2.10 (p. 45) presents values of critical domain diameters and domain wall energies for some materials.

Table 1.2 Exchange lengths for 3d metals (from Table 2.9, p. 45, Chap.2)

Element	l_{ex} (nm)
Fe	3.28
Co	4.70
Ni	7.64

1.2.2 Broken Translation Symmetry

Every finite crystal has frontiers where the translational symmetry is lost or broken. In solids of nanometric size, a significant proportion of the atoms are on or near these frontiers. The absence of translation symmetry brings about several important consequences to the physical properties of these systems.

Three aspects of the problem of symmetry breaking will be discussed: a) the relation of the physical properties of the samples to their dimensionality (samples with quasi-zero dimension ($0D$), unidimensional ($1D$), bidimensional ($2D$), or tridimensional ($3D$)); b) the change in coordination of the atoms at the interface; and c) the effect of the increase in the proportion of surface (or interface) atoms in nanoscale samples.

1.2.2.1 Dimensionality and Density of Electronic States

The electronic band structure of a solid depends on its dimensionality. This can be exemplified in the simplest description of a conducting solid, the free electron model, in which the electrons are treated as a gas (called a Fermi gas) only subject to the infinite potentials at the walls of the container. An electron gas in a limited spatial region will show an availability of electronic states (measured by its density of states $D(E)$) that depends on the dimensionality of this region: If it is in one dimension or two dimensions, $D(E)$ will differ from the three-dimensional case. The effects of the difference in dimensionality may be shown through the differences in $D(E)$ and are summarized in Fig. 1.2.

Let us examine initially a Fermi gas in three dimensions; we wish to obtain the form of the density of states $D(E)$. The electrons are supposed to be in a container with three dimensions and infinitely high walls; there are no interactions between the electrons.

Let us consider that the potential $V(x, y, z)$ inside the box of side L is V_0 =const for $0 \leq x \leq L$, $0 \leq y \leq L$, and $0 \leq z \leq L$; $V = \infty$ otherwise.

The time-independent Schrödinger equation will be:

$$-\frac{\hbar^2}{2m}\nabla^2\psi(r) + V(r)\psi(r) = E'\psi(r)\ . \tag{1.6}$$

Using $E = E' - V_0(r)$, one obtains

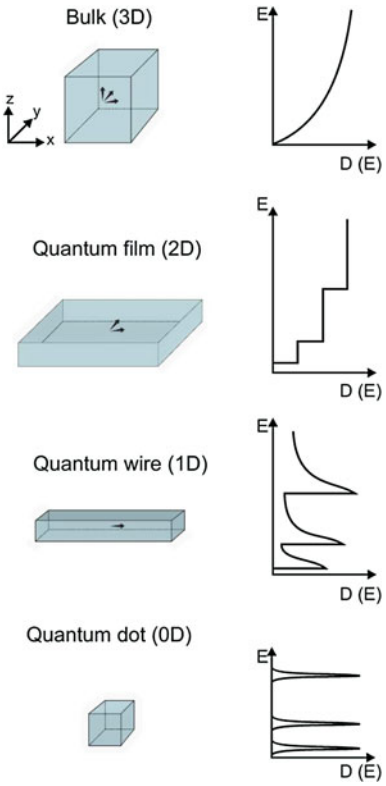

Fig. 1.2 Density of electronic states $D(E)$ as a function of energy for electrons, from *bottom* to *top*, in zero dimension, in one dimension, two dimensions, and three dimensions (based on [8])

$$-\frac{\hbar^2}{2m}\nabla^2\psi(r) = E\psi(r)\ . \tag{1.7}$$

Since the infinite potential at the walls forbids the presence of the electrons outside them, the boundary conditions for $\psi(r)$ will be: $\psi = 0$ for $x = 0$ and $x = L$, $y = 0$ and $y = L$ and $z = 0$ and $z = L$.

The solution of Schrödinger's equation, using these boundary conditions, will be:

$$\psi(r) = \left(\frac{2}{L}\right)^{3/2} \sin k_x x\ \sin k_y y\ \sin k_z z\ . \tag{1.8}$$

The corresponding energies are obtained by substituting $\psi(x)$ from (1.8) into 1.7:

$$E = \frac{\hbar^2}{2m}\left(k_x^2 + k_y^2 + k_z^2\right)\ , \tag{1.9}$$

where m is the electron mass and k_i are the components of its wavevector.

From the boundary conditions, one obtains:

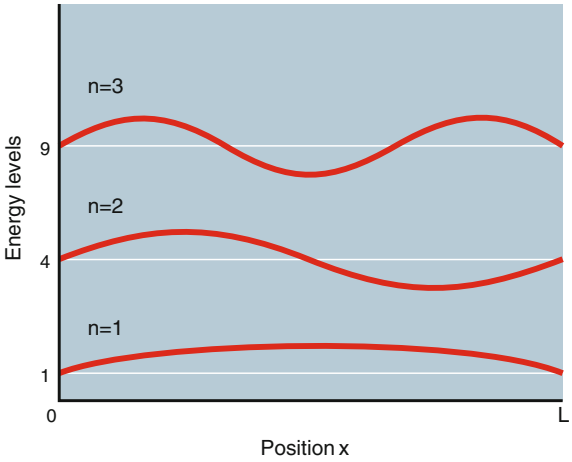

Fig. 1.3 Graph of E/E_0 (*dotted lines*) for the lower three energy levels and wavefunctions versus x (*continuous lines*) for a free electron gas confined to a one-dimensional box

$$k_x = \pm\frac{2\pi}{L}n_x, \qquad k_y = \pm\frac{2\pi}{L}n_y \qquad k_z = \pm\frac{2\pi}{L}n_z\ , \tag{1.10}$$

where n_x, n_y and n_z take values 1, 2, 3 ....

The wave functions for a free electron in a one-dimensional box, for the first three values of n, and the corresponding energies E are illustrated in Fig. 1.3. This figure shows the form of the first three lowest energy wave functions, as well as the corresponding energies E/E_0, where E_0 is the energy for the level with $n = 1$.

According to the Pauli exclusion principle, two electrons (spin up and spin down) occupy one state defined by (n_x, n_y, n_z). But how many states are there to be occupied? To count the number of states, one has to count the number of values of k.

At $T = 0$ K, all states are occupied up to k_F, the Fermi wavevector, in a volume $V_k = \frac{4}{3}\pi k_F^3$. Since each triplet (k_x, k_y, k_z) occupies a volume of $v = (2\pi/L)^3 = 8\pi^3/V$ in k-space, the number of states N will be

$$2\cdot\frac{V_k}{v} = 2\cdot\frac{\frac{4}{3}\pi k_F^3}{(2\pi/L)^3} = \frac{V}{3\pi^2}k_F^3 = N\ , \tag{1.11}$$

where V is the volume of the box, or the volume occupied by the electrons in real space; the factor 2 accounts for the existence of electrons with spin $m_s = +1/2$ and $m_s = -1/2$.

From this equation, one derives k_F, and substituting into the expression of the energy (refeq:Espsksps), one obtains the Fermi energy E_F:

$$E_F = \frac{\hbar^2}{2m}\left(\frac{3\pi^2 N}{V}\right)^{2/3}\ . \tag{1.12}$$

This allows writing N as a function of E_F. The derivative of the expression obtained for N is the density of electron states at the Fermi level $D(E_F)$:

$$D(E_F) \equiv \frac{dN}{dE_F} = \frac{V}{2\pi^2}\left(\frac{2m}{\hbar^2}\right)^{3/2} E_F^{1/2} \,. \tag{1.13}$$

This result is the density of electron states at the Fermi level for the free electron gas contained in a three-dimensional box. The bidimensional and the one-dimensional densities of states may be derived, using in (1.11) the corresponding expressions for the volume of the box, total volume in k-space V_k, and volume per point in k-space in two and one dimensions. In two dimensions, $V_k = \pi k^2$, the volume per point is $(2\pi/L)^2$ and the volume of the box is L^2.

In one dimension, the total volume in k-space is $V_k = 2k$, the volume per point is $(2\pi/L)$, and the volume of the box is L. Consequently, the general expression for the density of states is:

$$D(E) = \left(\frac{2m}{\hbar^2}\right)\frac{V_k}{v}\frac{p}{k^2} \,, \tag{1.14}$$

where $p = 1, 2, 3$ for the corresponding dimensionalities, as can be verified (Exercise 1.2). Substituting, one obtains the densities of states for the different dimensionalities.

In three dimensions:

$$D(E) = V\frac{1}{2\pi^2}\left(\frac{2m}{\hbar^2}\right)^{3/2} E^{1/2} \,. \tag{1.15}$$

In two dimensions:

$$D(E) = V\frac{1}{2\pi}\left(\frac{2m}{\hbar^2}\right) \,. \tag{1.16}$$

Note that in this case, the density of states $D(E)$ does not depend on the energy, and it is a constant.

And finally, in one dimension,

$$D(E) = V\frac{1}{\pi}\left(\frac{2m}{\hbar^2}\right)^{1/2} E^{-1/2} \,. \tag{1.17}$$

These expressions for the densities of states of the free electron gas for different dimensions (1, 2 and 3) are represented in the graphs of Fig. 1.4.

We will now discuss what happens if the object that contains the electrons is a solid of nanometric dimensions. There will be quantum confinement in any case where one or more dimensions of the volume that contains the electron gas are comparable to λ_F of the electron. In objects with dimensions comparable to this wavelength, the wave character of the electrons will be dominant, and their energies will be quantized.

To obtain the densities of states in the confined systems, one has to take into consideration the boundary conditions. The electrons may be confined in the three dimensions; i.e., they may be contained in an object that is nanometric in the three

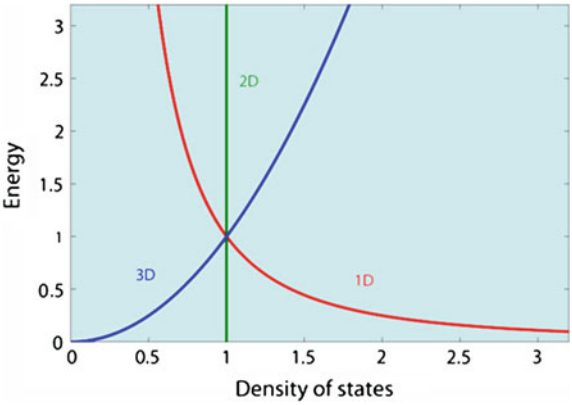

Fig. 1.4 Normalized densities of electronic states $D(E)/C_p$ (where C_p is a constant factor for each dimensionality p) as a function of energy, for different dimensionalities, $1D$, $2D$, and $3D$

dimensions—this is the case of a quantum dot. If the electrons are confined in two dimensions, i.e., if the third dimension is macroscopic, one has a quantum wire or a nanowire. If the electrons are confined in one dimension, one has a quantum well or a quantum film. If the electrons are not confined in any dimension, one has a macroscopic object.

(1) Object confined in three dimensions, or zero-dimensional object (quantum dot):

The allowed values for the energy of the electrons are given by (1.9). The energies of the different levels depend on k_x, k_y, and k_z. The condition of infinite potential at the walls implies $k_x = n_x\pi/L_x$, $k_y = n_y\pi/L_y$, and $k_z = n_z\pi/L_z$, where L_x, L_y, and L_z are the dimensions of the box where the electrons are contained.

$$E = \frac{\hbar^2\pi^2}{2m}\left(\frac{n_x^2}{L_x^2} + \frac{n_y^2}{L_y^2} + \frac{n_z^2}{L_z^2}\right). \tag{1.18}$$

The separation between the energy levels is given by dE_k. One assumes to simplify $L_x = L_y = L_z = L$, and also $n_x = n_y = n_z = n$. For a nanoscale solid with $L = 1$ nm, the energy levels are separated by $dE = 3\hbar^2\pi^2/mL^2 \sim 1$ eV. Therefore, the energy spectrum is formed of discrete levels, similar to the atomic levels, with energies given by

$$E_n = \frac{3\hbar^2\pi^2}{2mL^2}n^2. \tag{1.19}$$

The density of states curve $D(E)$ is formed of a series of delta functions at the energies E_n.

(2) Object confined in two dimensions, and free in one dimension (quantum wire or nanowire):

One may assume that the object is macroscopic in the z direction, and the dimensions $L_x = L_y$ are nanoscopic.

From (1.18), taking $L_z = L$ and $n_z = n$, one obtains

$$E = \frac{\hbar^2 \pi^2}{2m} \left(\frac{n_x^2}{L_x^2} + \frac{n_y^2}{L_y^2} + \frac{n^2}{L^2} \right) . \tag{1.20}$$

In this case, the separation between the energy levels labeled by n_x and n_y remains large, of the order of eV. The separation of the levels corresponding to n is much smaller, since L is a number typically $10^7 - 10^9$ times larger than the x and y dimensions. One may consider these levels as occupying a practically continuous range of values. $E(k)$ is then given by parabolas displaced by $\hbar^2 \pi^2 / 2mL^2$.

The density of states curve $D(E)$ is formed of a series of peaks at the values of E_n; above each peak there exists a region with a continuous dependence with E.

(3) Object confined in one dimension and free in two dimensions (quantum film or quantum well):

If the confinement is limited to the x-axis, the electrons are free to move in the directions of the plane (y and z axes) and the energy levels are given (for $L_y = L_z = L$) by:

$$E = \frac{\hbar^2 \pi^2}{2m} \left(\frac{n_x^2}{L_x^2} + 2\frac{n^2}{L^2} \right) . \tag{1.21}$$

In the same way as in the preceding case, the energies of the levels, labeled by n_x, exhibit a large difference. E versus k_x and k_y is given by parabolic surfaces displaced of $\hbar^2 \pi^2 / 2mL^2$. The density of states curve $D(E)$ is formed of a series of steps, within a parabolic envelope.

(4) Object without confinement, electrons free to move in the three directions (macroscopic object):

Taking the frontiers defined by $L_x = L_y = L_z = L$ as macroscopic lengths, the energies are given by:

$$E = \frac{\hbar^2 \pi^2}{2m} \left(3\frac{n^2}{L^2} \right) . \tag{1.22}$$

The energy levels are now distributed over a continuum of states, as shown in Fig. 1.4. The graph of E_k is represented by a parabolic surface, and the density of states curve $D(E)$ is the familiar parabola shown in Fig. 1.4.

The density of states curves shown in Fig. 1.2 differ from those that appear in Fig. 1.4, since there are obvious steps or discontinuities in Fig. 1.2. These steps arise, for example, in the case of a $D2$ solid (quantum film or quantum well), from the electron confinement in the dimension perpendicular to the plane. This confinement induces the appearance of discrete levels in the density of states; the dependence $D(E) =$ constant is observed at the energies corresponding to these levels.

A simple visual examinatioin of the density of states curves $D(E)$ shown in Fig. 1.2 reveals important differences in this function. The appearance of $D(E)$ for the $0D$ sample is similar to the same function for atoms: $D(E)$ has narrow peaks, corre-

sponding to well-defined values of the kinetic energy of the conduction electrons. For this reason, quantum dots are often referred to as "artificial atoms."

The curve $D(E)$ for quantum wires ($1D$) also has narrow peaks, but in this case, there are electronic states that may be occupied for intermediate values of the energy E. The curve for a bidimensional $2D$ nanosystem shows some well-defined steps, and again, there exists a quasicontinuum of states that may be occupied in the whole range of energies. The result of $D(E)$ for a macroscopic system in the free electron approximation is the well-known parabola, applicable in the simplest description of the metals.

Many physical properties of a solid may be directly related to the electronic density of states $D(E)$, such as the Pauli susceptibility and the conduction electron contribution to the specific heat. The Pauli susceptibility that measures the response of the free electron gas to an applied magnetic field is given by:

$$\chi_P = \mu_0 \mu_B^2 D(E_F) \ , \tag{1.23}$$

where $D(E_F)$ is the density of states at the Fermi level.

The importance of the effect of low dimensionality on the properties of the conduction electrons can be estimated from the size of the nano-object relative to the Fermi wavelength. This wavelength can be computed from the expression relating N to k_F (1.11).

$$k_F = \left(\frac{3\pi^2 N}{V} \right)^{1/3} \ . \tag{1.24}$$

Using the electronic density $n = N/V$, the Fermi wavelength becomes:

$$\lambda_F = 2\pi \left(\frac{1}{3\pi^2 n} \right)^{1/3} \ . \tag{1.25}$$

Therefore the Fermi wavelength is inversely proportional to $n^{1/3}$, and consequently, this wavelength is much larger in semiconductors ($\sim$100 nm) than in the metals ($\sim$0.1 nm). For example, in Fe, the Fermi wavelength is $\lambda_F = 0.37$ nm.

The magnetic moments of the transition element atoms also depend on the dimensionality of the structures where they are found. This dependence is evident in the computed magnetic moments of Ni and Fe for different dimensionalities, given in Table 1.3. The iron magnetic moment, for example, varies from 2.27 μ_B, for a 3D solid, to 4.0 μ_B for 0D (free atom).

The charge and spin densities near surfaces and interfaces are modified, as is illustrated in Fig. 1.5, where there are shown the computed charge density in the Fe(001) surface of a thin film [29] and the spin density on an Fe(110) surface [41]. It is apparent that the charge and spin densities of the surface atoms are significantly different from the corresponding densities at the inner rows of atoms.

An additional circumstance that modifies the magnetic properties of nanoscale systems is the relevance of their immediate neighborhood, or physical systems in

Table 1.3 Computed magnetic moments (in μ_B) and dimensionality for Ni and Fe samples [35]

Element	Zero (0*D*)	One (1*D*)	Two (2*D*)	Three (3*D*)
Ni	2.0	1.1	0.68	0.56
Fe	4.0	3.3	2.96	2.27

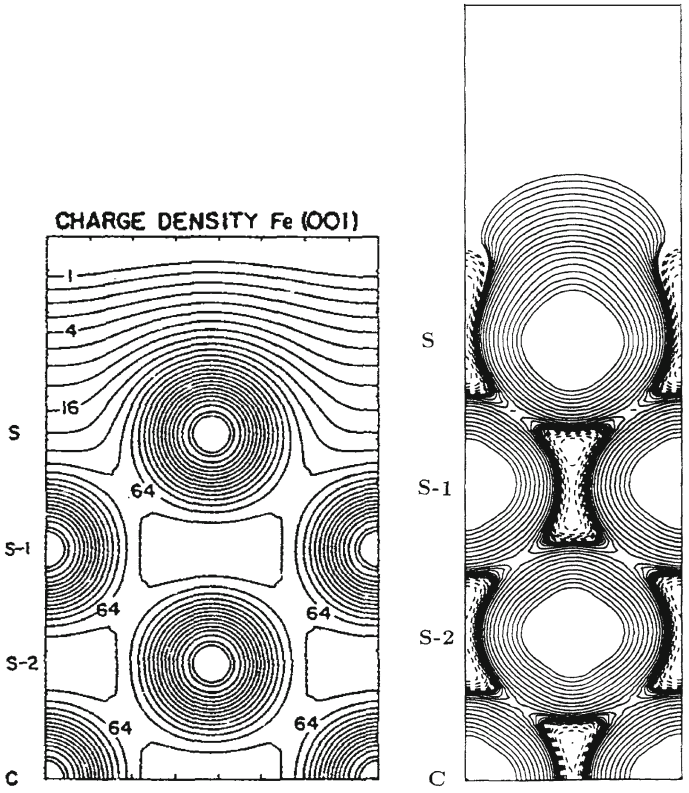

Fig. 1.5 *Left* representation of the computed conduction electron charge density at the surface of a seven-layer Fe(001) film, from each line to the next the density varies by a factor of $\sqrt{2}$ [29]. Reprinted figure with permission from [S. Ohnishi, A.J. Freeman, and M. Weinert, Phys. Rev. B, 28, p. 6742 1983]. Copyright (1983) by the American Physical Society; Right: total spin density for Fe(110) surface. *Solid* and *dashed lines* indicate positive and negative spin density, respectively [41]. Reprinted figure with permission from [Ruqian Wu and A. J. Freeman, Phys. Rev. Lett., 69, p. 2868, 1992]. Copyright (1992) by the American Physical Society

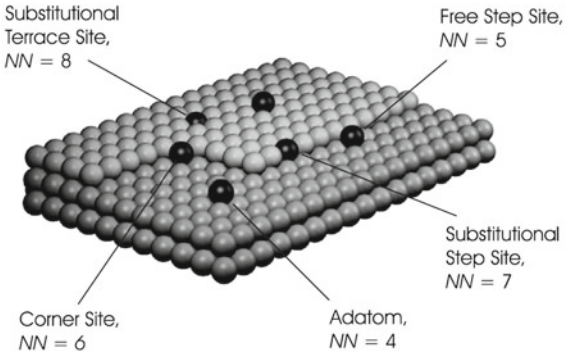

Fig. 1.6 Atomic sites on a thin film showing the different coordination numbers. The number *NN* of nearest neighbors of the atoms on the surface (adatom, $NN = 4$), atom near a step ($NN = 5$), atom in the step ($NN = 7$), and finally, a substitutional atom at the surface ($NN = 8$). (Reproduced with permission from [32])

close contact. This is the case of magnetic thin films that are deposited on substrates or are covered with protective capping layers. For example, films of Co deposited on Cu(001) have Curie temperatures that vary a few degrees, in an oscillatory way, with the thickness of a Cu capping layer [37].

1.2.2.2 Dimensionality and Reduced Coordination Number

An effect related to the broken translation symmetry at surfaces is that atoms in these regions have a reduced number of neighbors, as compared to atoms in the bulk of the sample. Let us take as an example the interface between two regions, one formed of atoms *A* and the other of atoms *B*. The *A* atoms at the interface may have the same number of nearest neighbors as in the macroscopic sample, but there, of course, they will have a different neighborhood, formed of atoms *A* and *B*.

The atoms at the boundary of the sample, for instance, at the interface sample-vacuum, are surrounded by a smaller number of neighbors: They may have one neighbor less, two less, and so on. These surface atoms may be at a plane surface, at the corner of a step, or inside a step. An illustration of these different surroundings is given in Fig. 1.6. The figure shows atoms on different locations of the same surface, atoms with 4, 5, 6, 7, and 8 near neighbor atoms, i.e., coordination numbers 4, 5, 6, 7, and 8.

In general, the electronic structure of the atoms with a smaller coordination number is different from that of the atoms in the bulk. The density of states shows that the reduction in the coordination number results in a narrowing of the electronic bands (e.g., [9]). This effect is illustrated in Fig. 1.7, with densities of states of bulk metals compared to those of atoms on a (100) surface. For Fe, Co, and Ni, the (100) surface atoms exhibit narrower density of states curves, compared to those of bulk samples of the same materials.

The increasing orbital contribution to the magnetic moment with decreasing dimensionality is made evident from measurements made on Co in Pt, as illustrated on Table 1.4; the increase in anisotropy energy is also apparent.

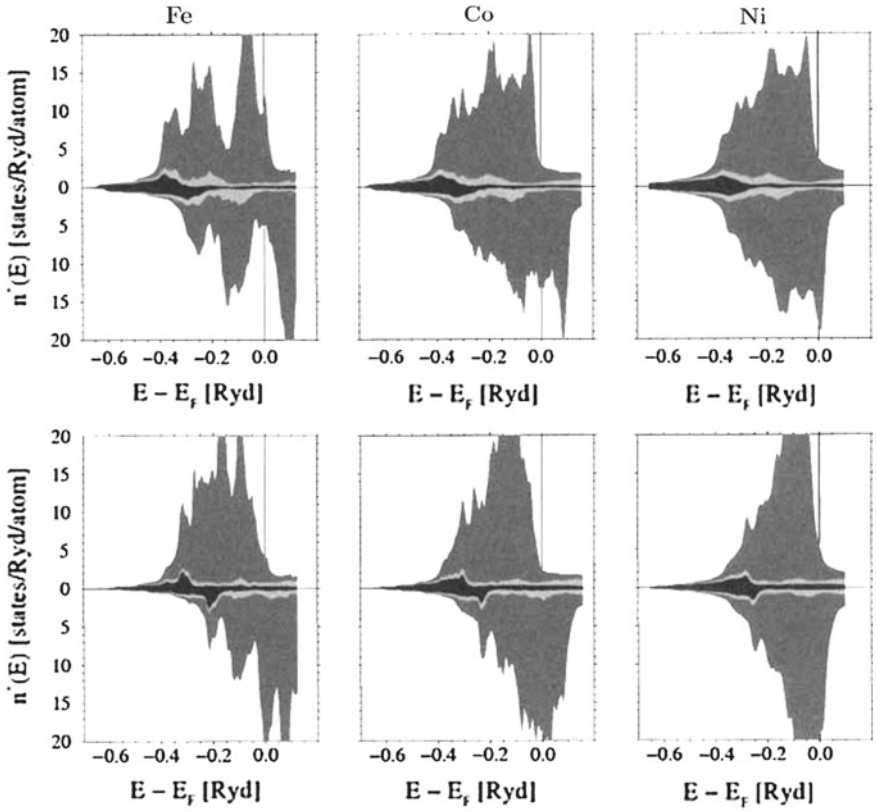

Fig. 1.7 Density of states for Fe, Co, and Ni in bulk metals (*above*) and on a (100) surface (*below*), showing the narrowing of the electronic bands in the latter case. The darkest areas represent the contribution of s electrons, the lightest p, and the intermediate d electrons. Reprinted with permission from [27]

The atoms located on the interfaces also have the point symmetry at their sites reduced, an effect that leads to level splitting and modification of the magnitude of the atomic magnetic moments. In Fe thin films in contact with Cu, Pd, and Ag, for instance, the Fe atoms exhibit enhanced magnetic moments (e.g., [37]).

The magnetic properties of atoms in interfaces are also affected by the presence of defects and impurities, such as adsorbates; strain may also change these properties and modify the lattice parameters.

Also, materials in the form of small particles may present a crystal structure that is different from that observed in bulk samples. This is the case, for example, of metallic cobalt that changes from hcp (hexagonal close packed) to fcc (face centered cubic) for particle diameters below approximately 30 nm.

Table 1.4 Magnetic orbital moment and magnetic anisotropy energy of Co in Pt with different dimensionalities [17]

	Bulk	Monolayer	Diatomic wire	Monoatomic wire	Two atoms	Single atom
Orbital moment (μ_B/atom)	0.14	0.31	0.37	0.68	0.78	1.13
Anisotropy energy (meV/atom)	0.04	0.14	0.34	2.0	3.4	9.2

Table 1.5 Proportion of number of surface atoms in cubic nanoscale clusters [20]

Number of atoms on each side	Number of surface atoms	Total number of atoms	Ratio of surface atoms to total number
5	98	125	78.5
10	488	1,000	48.8
100	58,800	1×10^6	5.9
1,000	6×10^6	1×10^9	0.6

1.2.2.3 Nanoscale Samples and Proportion of Surface Atoms

The role of surface atoms is determinant in catalytic processes. Catalysts are usually prepared in the form of finely divided powders, or porous matrices, since their activity relies on the contact of the substances that participate in the chemical reaction with atoms on their surface.

In the study of nanoscale samples, the contribution of the surface atoms to the physical properties increases with decreasing sample sizes. This is obvious, since the area of the surface of the samples varies typically as $\sim r^2$, while the volume of the samples varies as $\sim r^3$. As a consequence, the ratio of surface to volume varies roughly speaking as r^{-1}, therefore increasing with decreasing sample size. This is illustrated with the ratio of surface atoms to total number of atoms in cubic clusters, in Table 1.5. For example, a cube with 10 atoms of side has about half of the atoms on its surface.

The area per unit mass, or specific surface area, can be very large: For typical 2 nm spherical particles, this may be in the range of hundreds of square meters per gram.

In some limiting cases, as for example, in a thin film formed of only one or two atomic layers, every atom of the sample is a surface atom.

1.2.3 Nanomagnetic Samples and Dynamic Behavior

The dynamic behavior of the magnetization of nanomagnets may also be very different from that of macroscopic objects. This arises because, under the usual experimental conditions, thermal fluctuations play in this case a more important role. For example, in nanoscale magnetic particles, it is observed the phenomenon of superparamagnetism: In such particles, the magnetization inverts spontaneously, since the thermal energy $k_B T$ is comparable to their anisotropy energy (see Sect. 3.3, p. 82). A single-domain magnetic particle may spontaneously invert its magnetization; i.e., its direction may change from $+z$ to $-z$, if its temperature T is above a certain blocking temperature T_B. This effect has important implications, since if the magnetization of such particle were to be used for information storage, at $T = T_B$ the information would be lost. Therefore, in magnetic storage, with the reduction in physical size of the recorded bit, its thermal stability becomes more and more an important issue.

This phenomenon will be discussed in the chapter devoted to magnetic nanoparticles (Chap. 3).

Another physical process that depends on the dimensions, or on the dimensionality of the magnetic samples, is the motion of the magnetic domain walls. Magnetic domains are regions of constant magnetization in a magnetic solid, to be studied in Chap. 2, that are separated through a domain wall (DW). The motion of this wall is an important physical phenomenon that has recognized applications, as discussed in Sects. 2.4.3, 5.4, and 7.3.1 (pp. 58, 176 and 240). Studies of domain wall motion induced by an applied magnetic field or an applied current in a nanowire show that in both cases, there is a change in the behavior of the DWs as a function of the width of the nanowire; reducing this width there is a transition from 2D to 1D behavior. In the case of an applied field H, this occurs when the width reaches some few hundred nanometers, and the dependence of the domain wall velocity on the value of H changes, as one can see in Fig. 1.8 [23, 24].

1.3 Dimensionality and Critical Behavior

The change in magnetic behavior of the physical systems as a function of dimensionality is also reflected in the critical exponents that appear in the description of the divergences in the neighborhood of their critical temperatures.

Measurements of physical quantities in ferromagnetic samples at temperatures close to the transition temperature T_C – the Curie temperature – exhibit a power law dependence. From this dependence, there may be defined critical exponents, or critical indices. We therefore have for the specific heat C, for the saturation magnetization M_s, for the magnetic susceptibility χ and for the magnetic flux density or magnetic induction B:

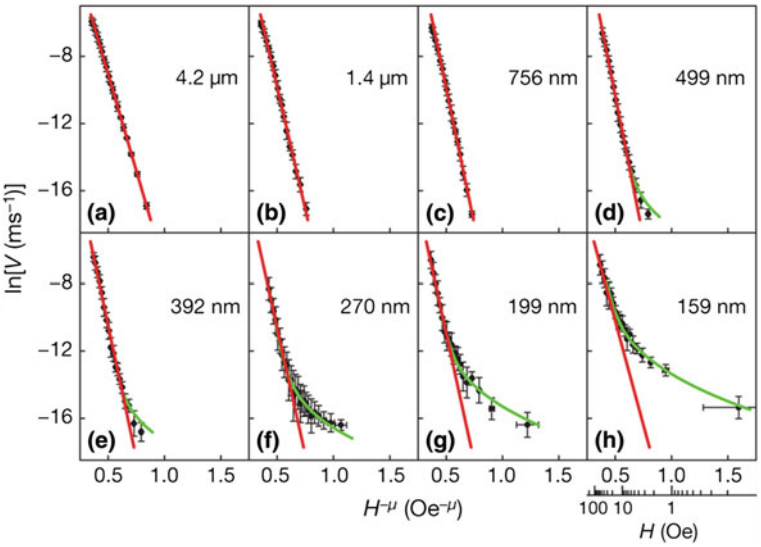

Fig. 1.8 Domain wall velocities for nanowires of different widths under applied field H, versus $H^{-1/4}$. The widths are: a) 4.2 μm, b) 1.4 μm, c) 756 nm, d) 499 nm, e) 392 nm, f) 270 nm, g) 199 nm and h) 159 nm. The straight lines are a fit appropriate to 2D criticality, whereas the curved line is fitted to a function for 1D criticality. Reprinted by permission from Macmillan Publishers Ltd: Nature, 458 07874, Copyright (2009) [23]

$$\begin{aligned} C &\sim |T - T_C|^{-\alpha} \\ M_s &\sim |T_C - T|^{\beta} \qquad (T < T_C) \\ \chi &\sim |T - T_C|^{-\gamma} \\ B &\sim M^{\delta} \qquad\quad (T = T_C) \end{aligned} \tag{1.26}$$

The experimentally measured values of the critical exponents for different magnetic systems are $\alpha \sim 0$, $\beta \sim 0.3$, and $\gamma \sim 1 - 2$.

In the Weiss model (mean field) description of ferromagnetism, the magnetization M can be written, in the case of magnetic ions with angular momentum $J = 1/2$, as

$$M = M_0 B_{1/2}(x) = M_0 \tanh\left(\frac{\mu_B B + \lambda_m M}{k_B T}\right), \tag{1.27}$$

where $B_{1/2}(x)$ is the Brillouin function, given by (2.6), on page 35. This equation can be rewritten as (for $M_0 = 1$)

$$\tanh^{-1}(M) = \frac{\mu_B B}{k_B T} + \frac{\lambda_m}{k_B T} M, \tag{1.28}$$

where λ_m is the molecular field parameter.

Table 1.6 Critical exponents in the mean field model, and values calculated numerically using a high-temperature expansion for three dimensions ($D = 3$) [4]

Magnitude	Exponent	Mean field	High T expansion ($D = 3$)
Specific heat	α	0	0.110 ± 0.005
Magnetization	β	$\frac{1}{2}$	0.312 ± 0.003
Susceptibility	γ	1	1.238 ± 0.002
Induction B	δ	3	5.0 ± 0.05

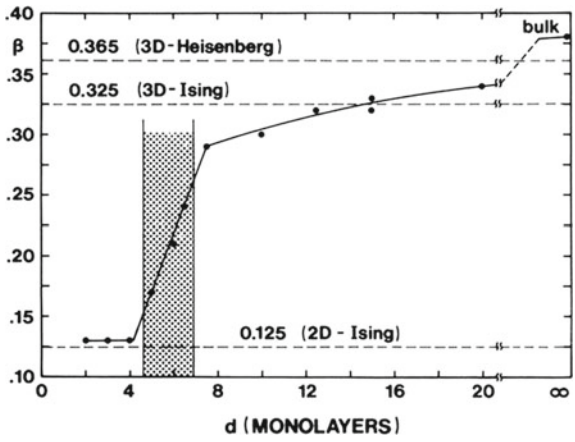

Fig. 1.9 Critical exponent β as a function of thickness, measured in number of monolayers, in thin films of Ni(111) on W(110), showing the transition from a bidimensional to a tridimensional behavior [25]. Reprinted figure with permission from [Yi Li and K. Baberschke, Phys. Rev. Lett., 68, p. 1209, 1992]. Copyright (1992) by the American Physical Society

For temperatures close to the critical temperature T_C, the magnetization will be small and we can expand the Brillouin function. From this expansion, one can determine (e.g., [4]) the critical exponents in the case of the mean field model (see Exercise 1.3) The exponents in this case are given at Table 1.6, together with values calculated numerically using a high-temperature expansion for dimensionality $D = 3$. In general, the agreement between the mean field critical exponents and the calculated values increases with increasing dimensionality.

Magnetization measurements as a function of temperature in mesoscopic and nanoscopic systems have been used to obtain critical exponents and, from these, verify the change in dimensionality as a function of their diameter, length, thickness, and so on. For example, in thin films, the transition from bidimensional to tridimensional behavior was observed (Fig. 1.9). For the thinnest samples of Ni films, the observed critical exponent is near 0.325, the value predicted for bidimensional systems (in the Ising model); as the thickness increases, the exponent changes, at about 6 monolayers, to a value close to that expected for tridimensional physical systems (0.365), in the same model [25]. The same effect was observed in Ni on Cu(111) and Ni on Cu(100) [21].

It is not easy to identify experimentally the effects of change in dimensionality on the magnetic properties of low-dimensional samples. For example, the variation

of magnetic ordering temperature T_C of thin films as a function of thickness may be related to the morphology of the films. Clusters may be formed in the process of film growth [37]; percolation of these clusters produces magnetic transitions, and at finite temperatures, smaller islands will exhibit superparamagnetic behavior.

If one atomic magnetic moment changes its direction, it will affect the direction of the moments of the neighbor atoms within a radius r. The correlation length ξ in magnetism can be understood in simple terms as associated with this radius. Another critical exponent relevant to the study of magnetic systems is the exponent ν that enters the expression of the temperature dependence of the correlation length ξ:

$$\xi \sim |T - T_C|^{-\nu} . \tag{1.29}$$

This exponent is related to the shift exponent λ that appears in the Curie temperature shift in geometrically confined samples. In this case, the relation between the Curie temperatures T_C of the low-dimensional system ($T_C(d)$) and T_C of the material in bulk form ($T_C(\infty)$) is:

$$\frac{(T_C(\infty) - T_C(d))}{T_C(\infty)} = \left(\frac{\xi}{d}\right)^{\lambda} . \tag{1.30}$$

In the above equation, d is the thickness of a thin film or the diameter of a particle, and $\lambda = 1/\nu$ is the displacement, or shift exponent, a number between 1.0 and 2.0. In mean field theory, $\lambda = 1$, and an estimate in the 3D Heisenberg model obtained $\lambda = 1.419 \pm 0.006$ [11]. An experimental study of maghemite nanoparticles resulted in a value of $\lambda = 1.1 \pm 0.2$ [18].

Further Reading

General

S.D. Bader, 'Colloquium: opportunities in nanomagnetism', Rev. Mod. Phys. **78** (2006) 1–15

X. Batlle and A. Labarta, 'Finite-size effects in fine particles: magnetic and transport properties', J. Phys. D: Appl. Phys. **35** (2002) R15–R42

C. Binns, 'Tutorial Section on Nanomagnetism', in *Nanomagnetism: Fundamentals and Applications*, Ed. C. Binns, (Elsevier, Oxford, 2014), pp. 1–32.

J.A.C. Bland and B. Heinrich, Eds., *Ultrathin Magnetic Structures*, volumes I–IV, (Springer, Berlin, 2005)

J.F. Bobo, L. Gabillet and M. Bibes, 'Recent advances in nanomagnetism and spin electronics', J. Phys.: Condens. Matter **16** (2004) S471–S496

C. Chappert and A. Barthelémy, 'Nanomagnetism and spin electronics', in *Nanoscience*, Ed. C. Dupas, P. Houdy and M. Lahmany, (Springer, Berlin, 2007), pp. 503–582

C.L. Dennis, R.P. Borges, L.D. Buda, U. Ebels, J.F. Gregg, M. Hehn, E. Jouguelet, K. Ounadjela, I. Petej, I.L. Prejbeanu and M.J. Thornton, 'The defining length scales of mesomagnetism: a review', J. Phys.: Condens. Matter **14** (2002) R1175–R1262

A. Enders, P. Gambardella and K. Kern, 'Magnetism of low-dimensional metallic structures', In *Handbook of Magnetism and Advanced Magnetic Materials*, Eds. H. Kronmüller and S. Parkin, (John Wiley & Sons, Chichester, 2007), vol. 1, pp. 577–639

M.R. Fitzsimmons, S.D. Bader, J.A. Borchers, G.P. Felcher, J.K. Furdyna, A. Hoffmann, J.B. Kortright, I.K. Schuller, T.C. Schulthess, S.K. Sinha, M.F. Toney, D. Weller, and S. Wolf, 'Neutron scattering studies of nanomagnetism and artificially structured materials', J. Magn. Magn. Mat. **271** (2004) 103–146

O. Fruchart and A. Thiaville, 'Magnetism in reduced dimensions', Compt. Rend. Phys. **6** (2005) 921–933

C.P. Poole, Jr. and F.J. Owens, *Introduction to Nanotechnology*, (John Wiley & Sons, Hoboken, 2003)

T. Shinjo, *Nanomagnetism and Spintronics*, 2nd edn. (Elsevier, Amsterdam, 2013)

R. Skomski, 'Nanomagnetics', J. Phys.: Condens. Matter **15** (2003) R841–R896

R.L. Stamps, S. Breitkreutz, J. Akerman, A. V. Chumak, Y. Otani, G.E.W. Bauer, J.-U. Thiele, M. Bowen, S.A. Majetich, M. Kläui, I.L. Prejbeanu, B. Dieny, N.M. Dempsey and B. Hillebrands, 'The 2014 Magnetism Roadmap', J. Phys. D: Appl. Phys. **47** (2014) 333001

C.A.F. Vaz, J.A.C. Bland and G. Lauhoff, 'Magnetism in ultrathin film structures' Rep. Prog. Phys. **71** (2008) 056501–78

R. Wiltschko and W. Wiltschko, 'The magnetite-based receptors in the beak of birds and their role in avian navigation', J. Comp. Physiol. A, **199** (2012) 1–10

Exercises

1.1 Characteristic lengths—In Table 1.1, there are given some characteristic lengths related to some physical properties of solid state matter. Compare the interatomic distance in Fe (2.5×10^{-1} nm) with a) the de Broglie wavelength of thermal neutrons at $T = 300$ K. Using the mass $m_N = 1.67 \times 10^{-27}$ kg, b), the de Broglie wavelength of an electron accelerated by a 10,000 V potential (rest mass $m_e = 9.11 \times 10^{-31}$ kg).

1.2 Volume in k space—Derive (1.14):

$$D(E) = \left(\frac{2m}{\hbar^2}\right) \frac{V_k}{v} \frac{p}{k^2}$$

where $p = 1, 2, 3$ for the corresponding dimensionalities.

1.3 Critical exponents—Obtain the critical exponents for the case of the mean field model.

1.4 Magnetic bacterium in the Earth field—A magnetic bacterium has a magnetic moment of 5×10^{-16} A m^2. What is the relation between the magnetic energy of the bacterium when its axis forms an angle of 60° to the Earth field ($\sim 0.5 \times 10^{-4}$ T) and the thermal energy $k_B T$ at room temperature?

References

1. C. Alexiou, R. Jurgons, Magnetic drug targeting, in *Magnetism in Medicine: A Handbook*, 2nd edn., ed. by W. Andrä, H. Nowak (Wiley, Weinheim, 2007), pp. 596–605
2. S.D. Bader, Colloquium: opportunities in nanomagnetism. Rev. Mod. Phys. **78**, 1–15 (2006)
3. X. Batlle, A. Labarta, Finite-size effects in fine particles: magnetic and transport properties. J. Phys. D: Appl. Phys. **35**, R15–R42 (2002)
4. M. Le Bellac, *Quantum and Statistical Field Theory* (Oxford University Press, Oxford, 1991)
5. C. Binns, Tutorial section on nanomagnetism, in *Nanomagnetism: Fundamentals and Applications*, ed. by C. Binns (Elsevier, Oxford, 2014)
6. J.A.C. Bland, B. Heinrich, *Ultrathin Magnetic Structures* (Springer, Berlin, 2005)
7. J.F. Bobo, L. Gabillet, M. Bibes, Recent advances in nanomagnetism and spin electronics. J. Phys. Condens. Matter **16**, S471–S496 (2004)
8. V.E. Borisenko, S. Ossicini, *What is What in the Nanoworld* (Wiley, Weinheim, 2004)
9. K.H.J. Buschow (ed.), *Concise Encyclopedia of Magnetic and Superconducting Materials*, 2 edn (Elsevier, Amsterdam, 2005)
10. C. Chappert, A. Barthelémy, Nanomagnetism and spin electronics, in *Nanoscience*, ed. by C. Dupas, P. Houdy, M. Lahmany (Springer, Berlin, 2007), pp. 503–582
11. K. Chen, A.M. Ferrenberg, D.P. Landau, Static critical behavior of three-dimensional classical Heisenberg models: a high-resolution Monte Carlo study. Phys. Rev. B **48**, 3249–3256 (1993)
12. C.L. Dennis, R.P. Borges, L.D. Buda, U. Ebels, J.F. Gregg, M. Hehn, E. Jouguelet, K. Ounadjela, I. Petej, I.L. Prejbeanu, M.J. Thornton, The defining length scales of nanomagnetism: a review. J. Phys. Condens. Matter **14**, R1175–R1262 (2002)
13. A. Enders, P. Gambardella, K. Kern, Magnetism of low-dimensional metallic structures, in *Handbook of Magnetism and Advanced Magnetic Materials*, vol. 1, ed. by H. Kronmüller, S. Parkin (Wiley, Chichester, 2007), pp. 577–639
14. M.E. Evans, F. Heller, *Environmental Magnetism* (Academic Press, San Diego, 2003)
15. M.R. Fitzsimmons, S.D. Bader, J.A. Borchers, G.P. Felcher, J.K. Furdyna, A. Hoffmann, J.B. Kortright, I.K. Schuller, T.C. Schulthess, S.K. Sinha, M.F. Toney, D. Weller, S. Wolf, Neutron scattering studies of nanomagnetism and artificially structured materials. J. Magn. Magn. Mater. **271**, 103–146 (2004)
16. P.P. Freitas, H. Ferreira, S. Cardoso, S. van Dijken, J. Gregg, Nanostructures for spin electronics, in *Advanced Magnetic Nanostructures*, ed. by D. Sellmyer, R. Skomski (Springer, New York, 2006), pp. 403–460
17. O. Fruchart, A. Thiaville, Magnetism in reduced dimensions. Comptes Rendus Phys. **6**, 921–933 (2005)
18. L. He, C. Chen, N. Wang, W. Zhou, L. Guo, Finite size effect on Néel temperature with Co_3O_4 nanoparticles. J. Appl. Phys. **102**, 103911–103914 (2007)
19. R. Hergt, W. Andrä, Magnetic hyperthermia and thermoablation, in *Magnetism in Medicine: A Handbook*, 2nd edn., ed. by W. Andrä, H. Nowak (Wiley, Weinheim, 2007), pp. 550–570
20. M. Hosokawa, K. Nogi, M. Naito, T. Yokoyama, *Nanoparticle Technology Handbook* (Elsevier, Amsterdam, 2007)
21. F. Huang, M.T. Kief, G.J. Mankey, R.F. Willis, Magnetism in the few-monolayers limit: a surface magneto-optic Kerr-effect study of the magnetic behavior of ultrathin films of Co, Ni, and Co-Ni alloys on Cu(100) and Cu(111). Phys. Rev. B **49**, 3962–3971 (1994)

22. J. Jorzick, C. Kramer, S.O. Demokritov, B. Hillebrands, B. Bartenlian, C. Chappert, D. Decanini, F. Rousseaux, E. Cambril, E. Sondergard, M. Bailleul, C. Fermon, A.N. Slavin, Spin wave quantization in laterally confined magnetic structures. J. Appl. Phys. **89**, 7091–7095 (2001)
23. K.-J. Kim, J.-C. Lee, S.-M. Ahn, K.-S. Lee, C.-W. Lee, Y.J. Cho, S. Seo, K.-H. Shin, S.-B. Choe, H.-W. Lee, Interdimensional universality of dynamic interfaces. Nature **458**, 740–742 (2009)
24. K.-J. Kim, J.-C. Lee, K.-H. Shin, H.-W. Lee, S.-B. Choe, Universal classes of magnetic-field- and electric-current-induced magnetic domain-wall dynamics in one and two dimensional regimes. Curr. Appl. Phys. **13**, 228–236 (2013)
25. Y. Li, K. Baberschke, Dimensional crossover in ultrathin Ni(111) films on W(110). Phys. Rev. Lett. **68**, 1208–1211 (1992)
26. A.S. Mathuriya, Magnetotactic bacteria for cancer therapy. Biotechnol. Lett. **37**, 491–498 (2015)
27. I. Mertig, Thin film magnetism: band calculations, in *Concise Encyclopedia of Magnetic and Superconducting Materials*, 2nd edn., ed. by K.H.J. Buschow (Elsevier, Amsterdam, 2005)
28. S. Odenbach, Ferrofluids, in *Handbook of Magnetic Materials*, vol. 16, ed. by K.H.J. Buschow (Elsevier, Amsterdam, 2006), pp. 127–208
29. S. Ohnishi, A.J. Freeman, M. Weinert, Surface magnetism of Fe(001). Phys. Rev. B **28**, 6741–6748 (1983)
30. P. O'Neill, Magnetoreception and baroreception in birds. Dev. Growth Differ. **55**, 188–197 (2013)
31. C.P. Poole Jr., F.J. Owens, *Introduction to Nanotechnology* (Wiley, Hoboken, 2003)
32. M.J. Prandolini, Magnetic nanostructures: radioactive probes and recent developments. Rep. Prog. Phys. **69**, 1235–1324 (2006)
33. T. Shinjo, *Nanomagnetism and Spintronics*, 2nd edn. (Elsevier, Amsterdam, 2013)
34. R. Skomski, Nanomagnetics. J. Phys.: Condens. Matter **15**, R841–R896 (2003)
35. S.N. Song, J. Ketterson, Ultrathin films and superlattices, in *Electronic and Magnetic Properties of Metals and Ceramics*, vol. 3A, ed. by R.W. Cahn, P. Haasen, E.J. Kramer (Wiley, New York, 1991)
36. R.L. Stamps, S. Breitkreutz, J. Akerman, A.V. Chumak, Y. Otani, G.E.W. Bauer, J.-U. Thiele, M. Bowen, S.A. Majetich, M. Kläui, I.L. Prejbeanu, B. Dieny, N.M. Dempsey, B. Hillebrands, The 2014 magnetism roadmap. J. Phys. D: Appl. Phys. **47**, 333001 (2014)
37. C.A.F. Vaz, J.A.C. Bland, G. Lauhoff, Magnetism in ultrathin film structures. Rep. Prog. Phys. **71**, 056501–056578 (2008)
38. D. Weller, T. McDaniel, Media for extremely high density recording, in *Advanced Magnetic Nanostructures*, ed. by D. Sellmyer, R. Skomski (Springer, New York, 2006), pp. 295–324
39. R. Wiltschko, W. Wiltschko, *Magnetic Orientation in Animals* (Springer, Berlin, 1995)
40. R. Wiltschko, W. Wiltschko, The magnetite-based receptors in the beak of birds and their role in avian navigation. J. Comp. Physiol. A **199**, 1–10 (2012)
41. R. Wu, A.J. Freeman, Spin density at the Fermi level for magnetic surfaces and overlayers. Phys. Rev. Lett. **69**, 2867–2870 (1992)

http://www.springer.com/978-3-319-59408-8

Principles of Nanomagnetism

Guimarães, A.P.

2017, XV, 330 p. 135 illus., 47 illus. in color., Hardcover
ISBN: 978-3-319-59408-8